A chemo-enzymatic method for preparation of saturated oligosaccharides from alginate and other uronic acid-containing polysaccharides

Mina Gravdahl [a], Olav A. Aarstad [a], Agnes B. Petersen [a], Stina G. Karlsen [a], Ivan Donati [b], Mirjam Czjzek [c], Ove Alexander Høgmoen Åstrand [d], Philip D. Rye [d], Anne Tøndervik [e], Håvard Sletta [e], Finn L. Aachmann [a,*], Gudmund Skjåk-Bræk [a]

[a] *Norwegian Biopolymer Laboratory (NOBIPOL), Department of Biotechnology and Food Science, NTNU Norwegian University of Science and Technology, Sem Sælands vei 6-8, N-7491 Trondheim, Norway*
[b] *Department of Life Sciences, University of Trieste, Via Licio Giorgieri 5, I-34127 Trieste, Italy*
[c] *Station Biologique de Roscoff (SBR), Sorbonne Université, CNRS, Integrative Biology of Marine Models (LBI2M), 29680 Roscoff, Bretagne, France*
[d] *AlgiPharma AS, Industriveien 33, Sandvika N-1337, Norway*
[e] *Department of Biotechnology and Nanomedicine, SINTEF Industry, Richard Birkelands vei 3B, 7034 Trondheim, Norway*

ARTICLE INFO

Keywords:
Alginate
Lyase
Uronic acid
NMR
Polygalacturonic acid
Heparin

ABSTRACT

Oligosaccharides from uronic acid-containing polysaccharides can be produced either by chemical or enzymatic degradation. The benefit of using enzymes, called lyases, is their high specificity for various glycosidic linkages. Lyases cleave the polysaccharide chain by an β-elimination reaction, yielding oligosaccharides with an unsaturated sugar (4-deoxy-L-*erythro*-hex-4-enepyranosyluronate) at the non-reducing end. In this work we have systematically studied acid degradation of unsaturated uronic acid oligosaccharides. Based on these findings, a method for preparing saturated oligosaccharides by enzymatic degradation of uronic acid-containing polysaccharides was developed. This results in oligosaccharides with a pre-defined distribution and proportion of sugar residues compared to the products of chemical degradation, while maintaining the chemical structure of the non-reducing end. The described method was demonstrated for generating saturated oligosaccharides of alginate, heparin and polygalacturonic acid. In the case of alginate, the ratio of hydrolysis rate of Δ-G and Δ-M linkages to that of G-G and M-M linkages, respectively, was found to be approximately 65 and 43, at pH* 3.4, 90 °C. Finally, this method has been demonstrated to be superior in the production of α-L-guluronate oligosaccharides with a lower content of β-D-mannuronate residues compared to what can be achieved using chemical depolymerization alone.

1. Introduction

Oligosaccharides can be produced from polysaccharides using different degradation methods, which may affect the distribution and proportions of monosaccharides, as well as their molecular size. Knowledge of the chemical structure of the oligosaccharides is a prerequisite for understanding their biological and physiological properties. Controlled and reproducible production of oligosaccharides is essential for optimizing their use in industrial applications such as pharmaceuticals, food, and biotechnology.

Alginates are a family of anionic and linear polysaccharides produced by brown algae and some bacteria (Gorin & Spencer, 1966; Linker & Jones, 1966) and consist of 1 → 4 linked β-D-mannuronic acid (M), and its C5-epimer α-L-guluronic acid (G). These uronic acid monomers can be arranged in three types of blocks of varying lengths: homopolymeric regions (G-blocks and M-blocks) and alternating regions (MG-blocks) (Haug, Larsen, & Smidsrød, 1967). The distribution and proportion of M and G in alginates impact the chemical and physical properties of the polysaccharide. Alginates containing G-blocks can form thermostable hydrogels in the presence of divalent cations, such as Ca^{2+}, explained by the so-called "egg-box" model (Grant, Morris, Rees, Smith, & Thom, 1973). G-blocks have shown to have antimicrobial effects

* Corresponding author.
E-mail addresses: mina.gravdahl@ntnu.no (M. Gravdahl), olav.a.aarstad@ntnu.no (O.A. Aarstad), agnes.b.petersen@ntnu.no (A.B. Petersen), stina.g.karlsen@ntnu.no (S.G. Karlsen), idonati@units.it (I. Donati), czjzek@sb-roscoff.fr (M. Czjzek), alexander.aastrand@algipharma.com (O.A.H. Åstrand), phil.rye@algipharma.com (P.D. Rye), anne.tondervik@sintef.no (A. Tøndervik), havard.sletta@sintef.no (H. Sletta), finn.l.aachmann@ntnu.no (F.L. Aachmann), gudmund.skjak-brak@ntnu.no (G. Skjåk-Bræk).

(Powell et al., 2023; Pritchard et al., 2016; Pritchard et al., 2017), as well as an effect on mucus thickness and detachment of cystic fibrosis (CF) mucus by calcium chelation (Ermund et al., 2017). Furthermore, G-blocks have also been used to make G-block-based diblocks to prepare defined nanoparticles (Solberg, Mo, Aachmann, Schatz, & Christensen, 2021), as well as other types of G-block-based conjugates (Solberg et al., 2022). A method for production of α-L-guluronate oligosaccharides with a lower content of β-D-mannuronate residues is therefore highly desirable.

Heparin is a highly sulfated negatively charged linear polysaccharide composed of uronic acids (β-D-glucuronic acid (GlcA) or L-iduronic acid (IdoA)) and α-D-glucosamine (GlcN) linked by 1,4-linkages. Heparin is clinically used as an anticoagulant (blood thinner) to prevent the formation of blood clots (Casu & Lindahl, 2001; Shriver, Capila, Venkataraman, & Sasisekharan, 2012; Wardrop & Keeling, 2008). Pectin is a large and structurally complex family of polysaccharides usually produced from fruit processing waste such as citrus peel or apple pomace and is primarily used in the food industry as gelling agents. Pectin consists of several structural modules, each of which may be isolated after enzymatic degradation and fractionation. One of the most common sugars in pectin is 1 → 4 linked α-D-galacturonic acid (GalA). The linkages in poly GalA are diaxial, resembling the G-G linkages in alginate, and can bind calcium ions and form junctions leading to gelation (Caffall & Mohnen, 2009).

Enzymes that cleave specific glycosidic linkages are invaluable tools for obtaining oligosaccharides with a precise distribution and proportion of sugar residues. Polyuronides are degraded by one family of enzymes: the lyases, which cleave the polymer chain through a β-elimination reaction resulting in oligosaccharides with an unsaturated sugar on the non-reducing end. Alginate lyases can be M-M, M-G, G-M, and/or G-G specific and *endo-* or exoacting. Endolytic alginate lyases cleave internal glycosidic bonds in alginates creating oligosaccharides of various lengths with an unchanged saturated uronate at the reducing end and an unsaturated 4-deoxy-L-*erythro*-hex-4-enepyranosyluronate residue (denoted Δ) at the non-reducing end (Fig. 1.) (Aarstad, Tøndervik, Sletta, & Skjåk-Bræk, 2012).

Exolytic alginate lyases react from the end of the chain, gradually converting alginate to short unsaturated oligosaccharides or Δ monosaccharides, which in an aqueous solution at neutral or alkaline pH, will spontaneously convert to hydrated 4-deoxy-L-*erythro*-5-hexulosuronate (DEH). Furthermore, Arntzen et al. (2021), discovered that DEH aldohydrate is further converted to two 5-member hemiketal ring epimers (4-deoxy-D-*manno*-(*5S*)-hexulofuranosidonate hydrate and 4-deoxy-D-*manno*-(*5R*)-hexulofuranosidonate hydrate) through intramolecular cyclization in aqueous solutions (pH 5.6).

The benefit of using enzymatic degradation instead of acid hydrolysis for generation of oligosaccharides is the enzymes' specificity towards the various glycosidic linkages, allowing production of oligosaccharides with defined sequences. Enzymatic degradation, usually performed under mild conditions (low temperature, pH 6–8), results in a narrower distribution of oligosaccharide lengths, has a high reaction rate, and produces high yields (Falkeborg et al., 2014). On the contrary, acid hydrolysis of polysaccharides to oligosaccharides can be time consuming, and the high temperature over a longer period may result in a complex series of caramelization reactions, resulting in brown pigments (Coultate, 2016). For the above-mentioned reasons, a method that

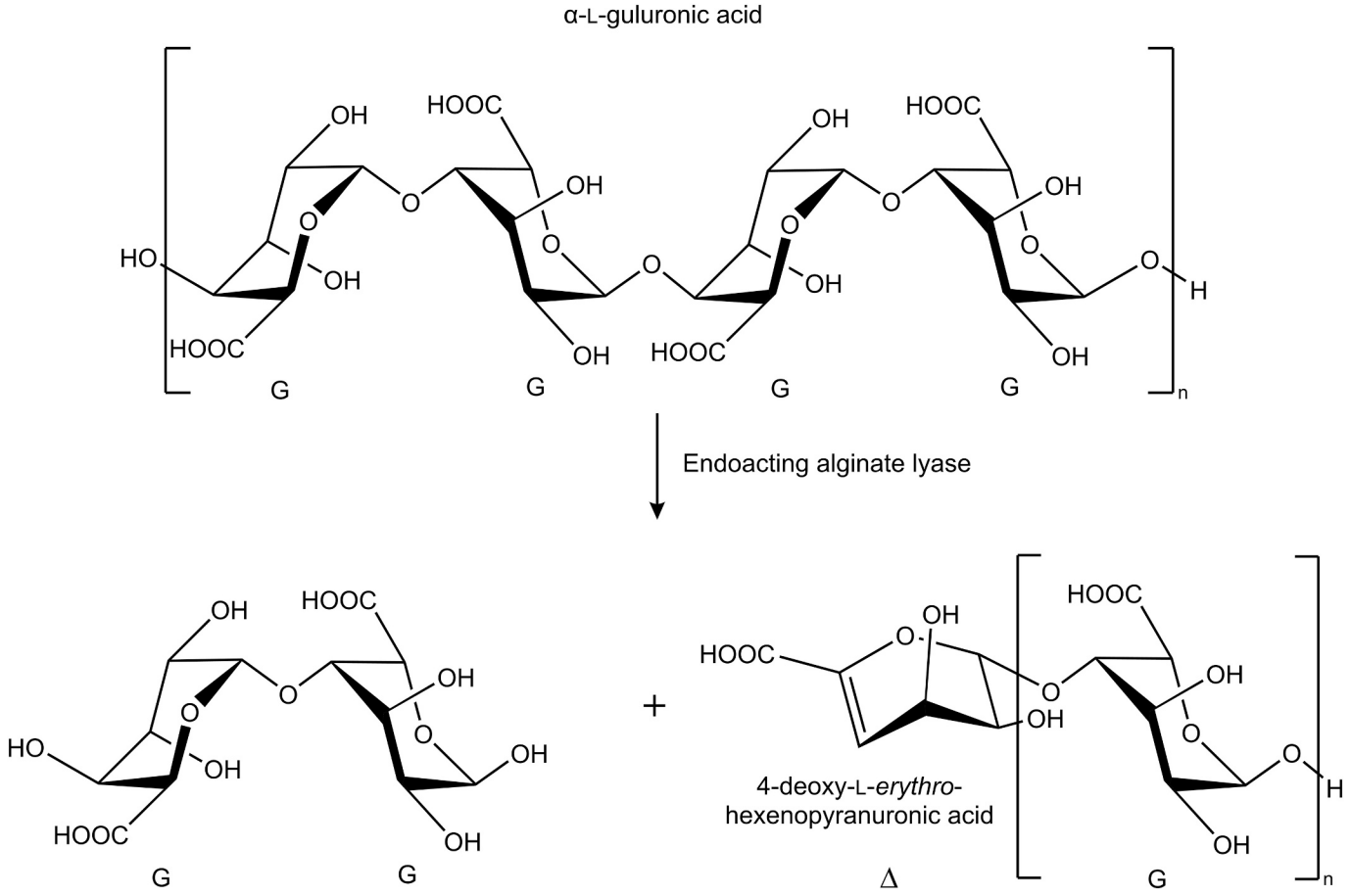

Fig. 1. Enzymatic degradation of an alginate G-block by an endoacting alginate lyase. After degradation, the alginate oligosaccharides will have an unsaturated residue (4-deoxy-L-*erythro*-hex-4-enepyranosyluronate, Δ) at the newly formed non-reducing end. In the four residues represented in this figure, the alginate structure changes from $GGGG_n$ to $GG + \Delta G_n$.

utilizes enzymatic degradation for preparation of oligosaccharides with a precise distribution and proportion of sugar residues without altering the chemistry of the non-reducing end is preferable.

Cleavage of a glycosidic linkage can occur through acid hydrolysis where water is a reagent. The first step in an acid hydrolysis reaction is protonation of the glycosidic oxygen. The linkage between C1 and the protonated oxygen is cleaved, leaving a carbocation formed at C1, which is resonance stabilized with the ring oxygen. The partial double bond changes the ring conformation. The carbocation reacts with water, and splits of a proton, resulting in a reducing sugar residue. The hydrolysis rate of different sugars depends on the chemistry of the sugar residues. When a polysaccharide has an unsaturated sugar at the non-reducing end, the intermediate structure contains two conjugated double bonds, which lowers the overall energy of the intermediate and increases its stability. Therefore, our hypothesis is that acid hydrolysis of a glycosidic linkage consisting of an unsaturated sugar at the non-reducing end has a higher reaction rate compared to the hydrolysis of a glycosidic linkage between two saturated uronic acid sugar residues.

The mechanism of hydrolysis of M-, G- and MG-enriched alginate fragments has been studied at pH values above 2, which show the order of selectivity; M-M linkages ≈ G-M linkages > M-G linkages > G-G linkages (Holtan, Zhang, Strand, & Skjåk-Bræk, 2006; Smidsrød, Haug, & Larsen, 1966; Smidsrød, Larsen, & Haug, 1967; Smidsrød, Larsen, Painter, & Haug, 1969). The mechanism of hydrolysis of a glycosidic linkage with a Δ on the non-reducing end has not been explored. In this work, we suggest a method for preparing saturated oligosaccharides after enzymatic degradation of uronic acid-containing polysaccharides and it is, to our knowledge, the first study describing this method. The described method has been tested on alginate (G-blocks and M-blocks), heparin, and polygalacturonic acid.

2. Material and methods

2.1. Optimum hydrolysis temperature for removal of unsaturated residues

Monodisperse oligomer fractions of unsaturated α-L-guluronic acid trimers (ΔGG) and unsaturated β-D-mannuronic acid trimers (ΔMM) were made by fractionation of partially lyase degraded polyM and polyG (Aarstad et al., 2012; Aarstad, Strand, Klepp-Andersen, & Skjåk-Bræk, 2013) on three serially connected Superdex30columns (2.6 × 60cm) (Holtan, Bruheim, & Skjåk-Bræk, 2006). The fractions were desalted by passing the solutions through an AG50W cation exchange column followed by freeze drying on a Christ alpha 1–4 LD freeze dryer (Germany) with an Edwards RV 5 vacuum pump (UK). The fractions were further dissolved in 50 mM NaCl (0.1 mg/ml), and the pH was decreased to 3.6 by addition of HCl. Acid hydrolysis was performed at 60 °C, 80 °C and 90 °C on the ΔGG fraction to find the optimal temperature for selective removal of the unsaturated residue. Samples were collected at various time points during the hydrolysis and analyzed directly using high-performance anion-exchange chromatography (HPAEC-PAD) (Section 2.8.1). Acid hydrolysis was then performed at 90 °C on the ΔMM fraction and analyzed the same way as the ΔGG fraction.

2.2. Acid hydrolysis of enzymatically degraded guluronate (ΔoligoG)

OligoG (AlgiPharma AS, Sandvika, Norway, $F_G = 0.89$, $M_n = 3200$ g/mol) was dissolved (10 mg/ml) in buffer (1.5 % NaCl, 1 mM $CaCl_2$ in deionized water (18.2 MΩcm) from an Omnia ultrapure system (Stakpure, Germany), pH 7.5). AlyM (M-lyase) was added to a concentration of 0.05 U/mg OligoG, and the sample was incubated in room temperature (RT) overnight. The sample was acid precipitated, neutralized, and freeze dried, and then dissolved (10 mg/ml) in buffer (1.5 % NaCl, 1 mM $CaCl_2$ in deionized water, pH 7.5). AlyA (G-lyase) was added to a concentration of 0.05 U/mg OligoG and incubated at RT for 4 h. The pH was decreased to 3.8 by addition of HCl and the sample was stored at −20 °C. The sample was then thawed, and the pH was increased to 7 by addition of NaOH before freeze drying. 10.0 mg material (ΔoligoG) was dissolved in 600 μl D_2O and the pH* (the pH measured in a deuterated solution using a pH meter where the electrode was filled with H_2O) was decreased to 3.4 using DCl (10–100 mM). The sample was further acid hydrolyzed in an NMR tube at 90 °C. During the acid hydrolysis ^{1}H NMR spectra were recorded on a 600 MHz instrument (Section 2.8.2).

2.3. Acid hydrolysis of enzymatically degraded mannuronate (ΔoligoM)

PolyM ($F_G = 0.0$, $M_w = 121{,}000$ g/mol, $M_n = 45{,}000$ g/mol) was produced by cultivation of an epimerase negative AlgG mutant of *Pseudomonas fluorescens* as previously described by Gimmestad et al. (2003) and Tøndervik et al. (2020). 1 g PolyM was dissolved (2.5 mg/ml) in 0.5 % NaCl and pH adjusted to 6.9. M-M/G-M specific alginate lyase (1.1 ml, 2 U/ml) from *Haliotis tuberculata* was added to the solution. The solution was further incubated for 27.4 h at 30 °C, followed by heating to 95 °C for 5 min and freeze dried. 10.0 mg was dissolved in 600 μl D_2O and the pH* was decreased to 3.4 using DCl (10–100 mM). The sample was further acid hydrolyzed in an NMR tube at 90 °C. During the acid hydrolysis ^{1}H NMR spectra were recorded on a 400 MHz instrument (Section 2.8.2).

2.4. Acid hydrolysis of enzymatically degraded heparin

Sodium salt of lyase treated porcine mucosal heparin ($M_w \approx 20{,}000$ g/mol, M_w/M_n ratio = 1.1) was kindly provided by LEO Pharma A/S (Cork, Ireland/Ballerup, Denmark) and was used without further purification. 10.0 mg was dissolved in 600 μl D_2O and the pH* was decreased to 3.4 using DCl (10–100 mM). The sample was further acid hydrolyzed in an NMR tube at 90 °C. During the acid hydrolysis ^{1}H NMR spectra were recorded on a 600 MHz instrument (Section 2.8.2).

2.5. Acid hydrolysis of enzymatically degraded polygalacturonic acid

Polygalacturonic acid sodium salt (1 mg/ml) (from citrus fruit, Sigma Aldrich, 052 K3786) was dissolved in Tris-buffer (50 mM, pH 8.0) and degraded using pectate lyase (1.4 U/mg) (*Aspergillus* sp., Megazyme) for 1 h before stopping the reaction by heating the sample to 95 °C for 10 min. 10.0 mg was dissolved in 600 μl D_2O and the pH* was decreased to 3.4 using DCl (10–100 mM). The sample was further acid hydrolyzed in an NMR tube at 90 °C. During the acid hydrolysis ^{1}H NMR spectra were recorded on a 600 MHz instrument (Section 2.8.2).

2.6. Degradation of polyM using an exo-lyase followed by characterization using NMR

PolyM ($F_G = 0.0$, $M_w = 17{,}000$ Da) was dissolved (3 mg/ml) in 600 μl buffer (10 mM HEPES, 2 mM NaCl, pH 7.0, D_2O) and degraded using the exo-lyase AlyA3 (Jouanneau et al., 2021) (1.5 mg/ml buffer) for approximately 1 h (RT) while stirring. The pH was adjusted using DCl (10 mM) to pH* 3.6 to stop the reaction. 10.0 mg was dissolved in 600 μl D_2O and the pH* was decreased using DCl (10–100 mM) to 3.4. The sample was further acid hydrolyzed in an NMR tube at 90 °C. During and after the acid hydrolysis, ^{1}H NMR spectra were recorded on a 600 MHz instrument (Section 2.8.2).

2.7. Preparation of saturated guluronic acid oligosaccharides starting from poly mannuronic acid (polyM)

PolyM ($F_G = 0.0$, $M_w = 411{,}000$ Da) (for production details, see Section 2.3) was dissolved (0.25 % *w/v*) in 50 mM MOPS buffer, pH 6.9, with 2.5 mM $CaCl_2$ and 10 mM NaCl. The G-block forming mannuronan C5-epimerase AlgE6 encoded by *Azotobacter vinelandii* (Tøndervik et al., 2020) was added to a final polyM/enzyme ratio of 200 and incubated at 37 °C for 48 h to give a degree of epimerization of 51 % ($F_G = 0.51$). The reaction was quenched by addition of EDTA to a final concentration of

4 mM. The solution was dialyzed (14 kDa MWCO) against 50 mM NaCl followed by dialysis against deionized water until the conductivity was below 4 µS. The pH was adjusted to 7.0 using NAOH (0.1 M) before freeze drying (Aarstad et al., 2013). The epimerized polyM (50 mg) was dissolved 4.6 ml buffer (200 mM NH_4Ac, pH 7.2, with 50 mM NaCl), and incubated with an M-M/G-M specific alginate lyase from *Haliotis tuberculata* (0.4 ml, 2 U/ml) at 30 °C for 20 h. The lyase reaction was terminated by heating the solution at 95 °C for 10 min. The solution was dialyzed (14 kDa MWCO) against 50 mM NaCl followed by dialysis against deionized water until the conductivity was below 4 µS (Aarstad et al., 2012).

To remove short degradation products (M and MG dimer to hexamers), the lysate was acid precipitated at pH 2 and centrifugated. The precipitate was washed with 0.01 M HCl and centrifugated again. The precipitate was finally dissolved in deionized water by addition of 0.1 M NaOH to pH 7 and freeze dried. To obtain oligoG devoid of Δ at the non-reducing ends, the sample was dissolved in deionized water (1 mg/ml) and the pH adjusted to pH 3.6 using HCl (10–100 mM). The solution was hydrolyzed at 95 °C for 7 h, neutralized and freeze dried. A sample after each step, including the starting material, was analyzed using ^{1}H nuclear magnetic resonance (NMR). The ^{1}H NMR spectra were recorded at 82 °C on a 600 MHz instrument (Section 2.8.2).

2.8. Characterization techniques

2.8.1. HPAEC-PAD

High-performance anion-exchange chromatography (HPAEC) with pulsed amperometric detection (PAD) was performed on an ICS 5000+ system (Thermo Scientific) with a 4 × 250 mm IonPAc ASA4 main column and 4 × 50 mm AG4A guard column. Samples (0.1–1.0 mg/ml, 25 µl) were eluted at 24 °C with isocratic 0.1 M NaOH and a linear sodium acetate gradient of 8.75 mM/min. The flow rate was 1 ml/min. After the method, a 15 min equilibration step with 0.1 M NaOH and 10 mM sodium acetate was included. Partially lyase degraded or acid hydrolyzed polyM (F_G = 0.0) and G-block ($F_G \geq 0.94$) were used as standards. Waveform A was used for detection (Thermo Scientific). Data were collected and processed with Chromeleon (Thermo Scientific) 7.2 software.

2.8.2. NMR

Time-resolved ^{1}H NMR was performed to follow the acid hydrolysis reactions. The sample was prepared by dissolving 10.0 mg of the samples in 600 µl D_2O, adjusting the pH*, and transferring the sample to a 5 mm NMR tube. The sample was inserted into a BRUKER NEO 400 or 600 MHz instrument (Bruker BioSpin AG, Fälladen, Switzerland) equipped with a 5 mm iProbe TBO preheated to 90 °C. After sample insertion, the sample magnet was locked, tuned, and shimmed, and a 1D ^{1}H spectrum was recorded to check sample integrity and magnet performance. As the acid hydrolysis starts when the sample reaches high temperature, there was a delay from the start of reaction until starting recording of time-resolved spectra due to these preparations. The time-resolved spectrum was recorded using a pseudo-2D setup, acquiring a 1D ^{1}H spectrum with water suppression (noesygppr1d) every 5 min for 18 h total.

Spectra for further characterization of products from acid hydrolysis were recorded at 20 °C on a Bruker Avance III HD 800 MHz spectrometer using a 5 mm *Z*-gradient CP-TCI (H/C/N) cryogenic probe. For structural elucidation of reaction products, the following spectra were recorded: 1D proton with water suppression (noesygppr1d), ^{1}H—^{13}C HSQC (heteronuclear single quantum coherence) with multiplicity editing, ^{1}H—^{13}C H2BC (heteronuclear two bond coherence; h2bcetgpl3pr or h2bcetgpl3) and ^{1}H—^{13}C HMBC (heteronuclear multiple bond coherence; hmbcetgpl3nd) with suppression of one-bond correlations. ^{1}H signals were internally referenced to the water signal and ^{13}C signals were indirectly referenced to the water signal based on absolute frequency ratios (Wishart et al., 1995). The spectra were recorded using TopSpin 3.6 pl 7 or 4.0.8 software (Bruker BioSpin) and processed and analyzed with TopSpin 4.0.7 software (Bruker BioSpin). The 800 MHz, 600 MHz and 400 MHz NMR spectrometers are located at the NV-NMR-Center/Norwegian University of Science and Technology (NTNU).

3. Results and discussion

3.1. Reaction rate of hydrolysis of the Δ-G linkage is dependent on temperature

Unsaturated α-L-guluronic acid trimers (ΔGG) were acid hydrolyzed at different temperatures (pH 3.6, 60 °C, 80 °C and 90 °C) and the increase in GG production was studied to find a suitable temperature for acid hydrolysis reaction. Hydrolysis of the Δ-G linkage in the trimers results in GG dimers and hydrolysis of the G-G linkage results in ΔG dimers. HPAEC-PAD was used to measure the relative proportions of ΔGG, ΔG and GG over the course of the hydrolysis reaction. Fig. 2 depicts the decrease in ΔGG and corresponding increase in ΔG and GG as changes in relative area [%] of the peaks in HPAEC-PAD chromatograms over time (Fig. S1 and Table S1, supplementary material). The figure shows that GG production happens at a much faster rate than production of ΔG, as can be seen from the corresponding changes in the relative

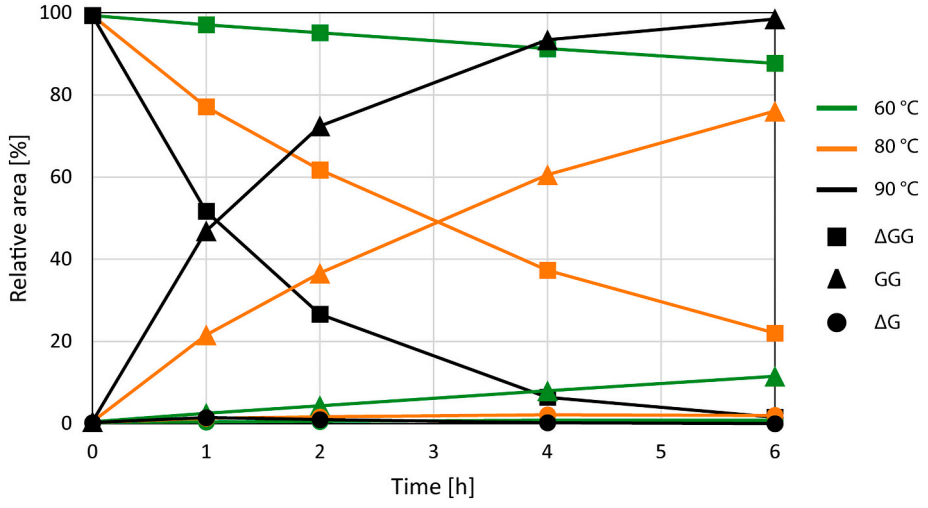

Fig. 2. Decrease in relative area [%] of the peak corresponding to ΔGG (filled square) and increase in relative peak area [%] of the peaks corresponding to GG (filled triangle) and ΔG (filled circle), in HPAEC-PAD chromatograms during acid hydrolysis (pH 3.6, 60 °C (green), 80 °C (orange), and 90 °C (black)).

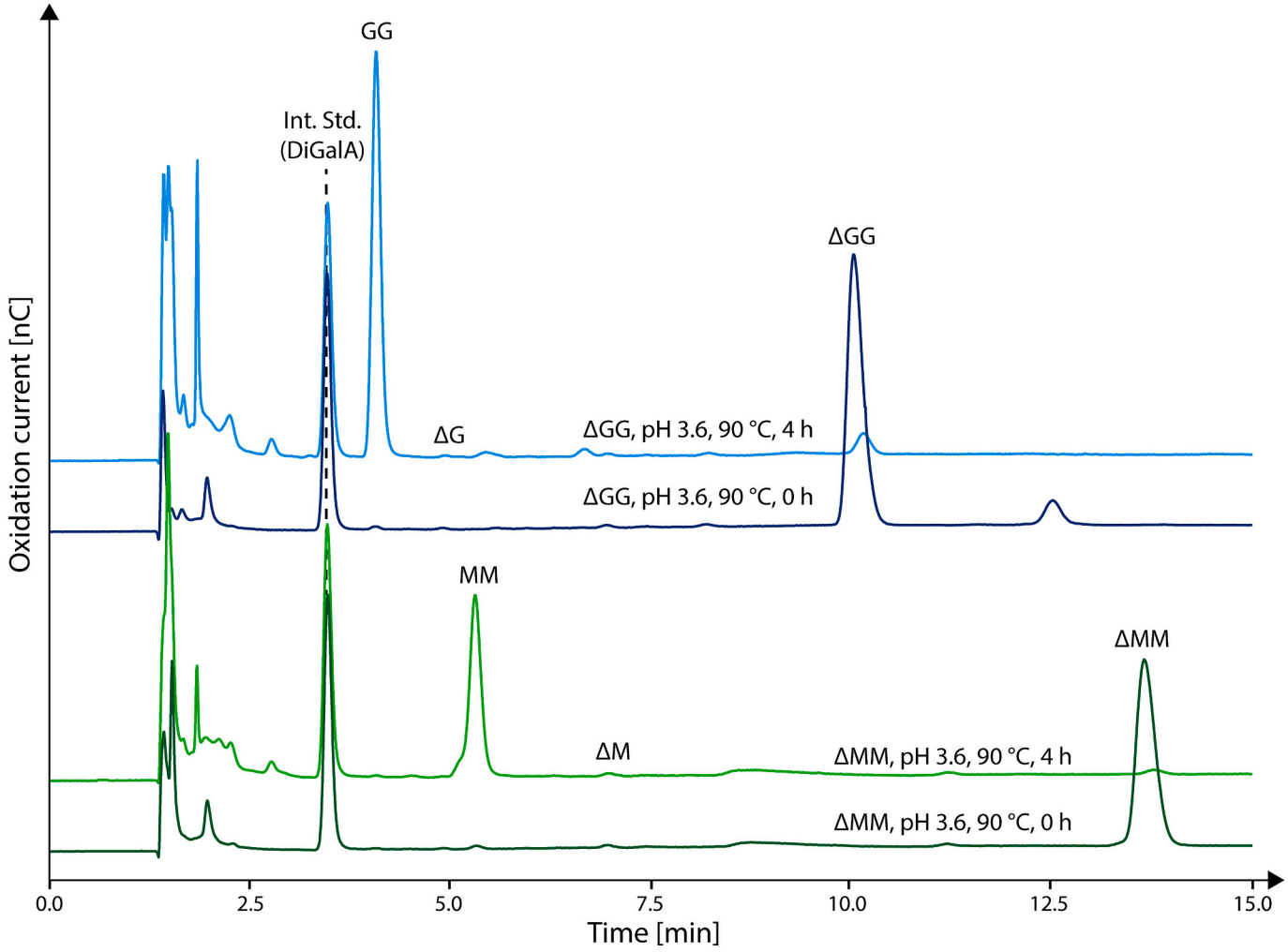

Fig. 3. Overlaid HPAEC-PAD chromatograms of ΔGG before (dark blue) and after (light blue) 4 h of acid hydrolysis at 90 °C, pH 3.6, and overlaid HPAEC-PAD chromatograms of ΔMM before (dark green) and after (light green) 4 h of acid hydrolysis at 90 °C, pH 3.6. The samples were separated on a Dionex IonPac AS4A column. Digalacturonic acid (DiGalA) was used as an internal standard (Int. Std.). The peaks eluting before 3 min correspond to monosaccharides (G or M and Δ) and salt (void fraction).

peak areas [%] for all temperatures. This indicates that the hydrolysis rate of the Δ-G linkage is faster compared to the hydrolysis rate of the G-G linkage for trimers, supporting our hypothesis. Furthermore, higher temperatures result in a comparatively faster hydrolysis reaction, while still maintaining the preferential cleavage of the Δ-G linkage. The greatest yields of GG production after 6 h of acid hydrolysis occurred at 90 °C, and all the following acid hydrolysis experiments in this study were therefore performed at temperatures $\geq$ 90 °C.

After establishing that the highest yields of GG from ΔGG were obtained at 90 °C after 6 h of acid hydrolysis, unsaturated β-D-mannuronic acid trimers (ΔMM) were acid hydrolyzed (pH 3.6, 90 °C) and analyzed using HPAEC-PAD during the hydrolysis reaction. HPAEC-PAD chromatograms of both ΔGG and ΔMM before and after 4 h acid hydrolysis (pH 3.6, 90 °C) are shown in Fig. 3 (Figs. S1-S2, supplementary material). The chromatograms depicted in Fig. 3 clearly show that also ΔMM is almost completely converted to MM, after 4 h of acid hydrolysis. This result further strengthens our hypothesis as the hydrolysis results in a higher production of MM compared to ΔM, meaning the hydrolysis rate of Δ-M linkages is higher compared to M-M linkages. Furthermore, Fig. 2 shows that approximately 6 % of the relative peak area of ΔGG remained after 4 h of acid hydrolysis, however in Fig. 3, approximately 3 % of the relative peak area of ΔMM remained after 4 h of acid hydrolysis. Hence, the hydrolysis of ΔMM seems to be slightly faster compared to the hydrolysis of ΔGG. The peaks eluting before 3 min in the HPAEC-PAD chromatograms corresponds to monosaccharides and salt. Finally, the same experiment was performed on a disperse ΔoligoG sample (Fig. S3, supplementary material), which showed an increase in the peak areas corresponding to saturated oligosaccharides (oligoG) and a decrease in the peak areas corresponding to unsaturated oligosaccharides (ΔoligoG).

3.2. *Estimation of rate constants for the hydrolysis of the glycosidic linkages using time-resolved ^{1}H NMR analysis*

To determine the rate constants (k) for acid hydrolysis of the different glycosidic linkages (Δ-G, G-G, Δ-M, M-M), experiments using time-resolved ^{1}H NMR were performed. ΔoligoG and ΔoligoM were separately acid hydrolyzed (pH* 3.4, 90 °C) in NMR tubes and a ^{1}H NMR spectrum was recorded every five minutes during the reactions. The large number of spectra recorded during the hydrolysis of ΔoligoG and ΔoligoM allowed for detailed analysis of the reaction kinetics. The rate constants were calculated from changes in ^{1}H NMR resonances of H-4 Δ, H-1 internal residues and α and β reducing end signals as a function of time until the integration value of the H-4 Δ signal reached

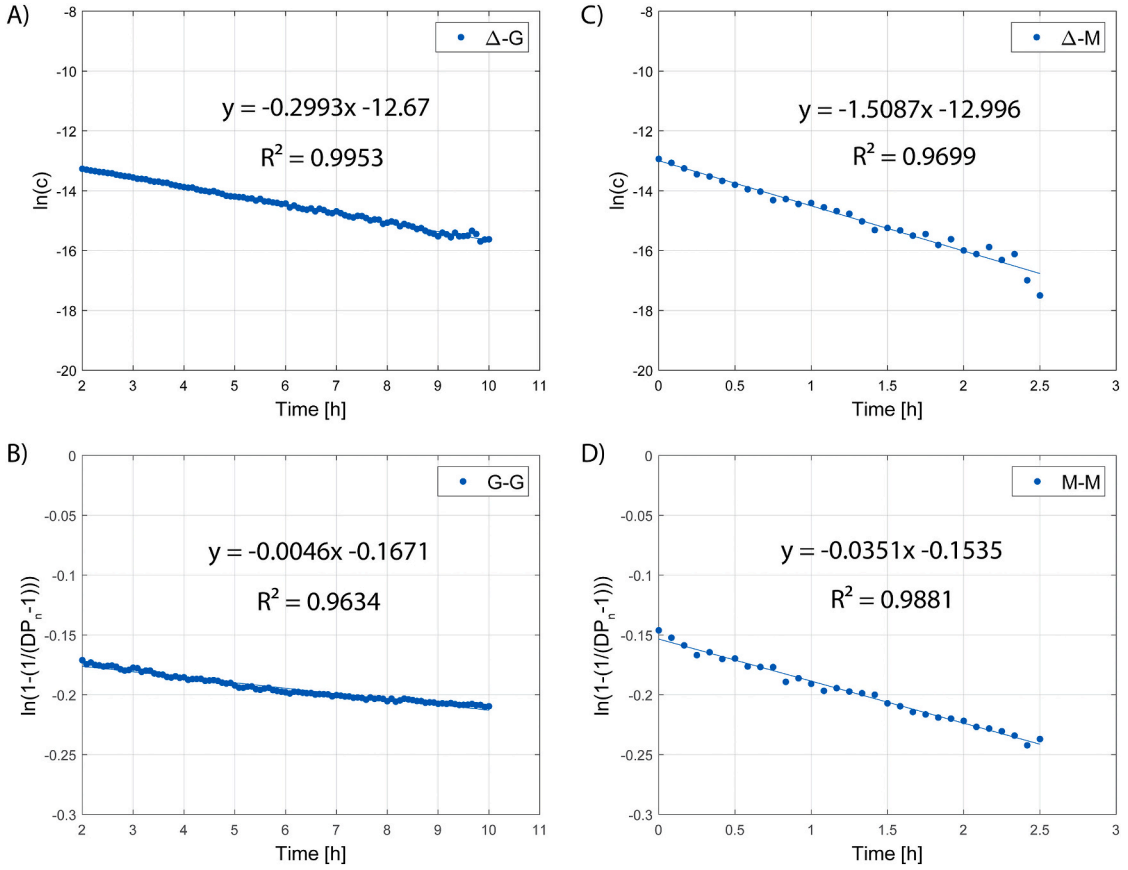

Fig. 4. Rate of degradation of A) Δ-G, B) G-G, C) Δ-M, and D) M-M glycosidic linkages in ΔoligoG (A and B) and ΔoligoM (C and D) at pH* 3.4, 90 °C. The respective rate constants, $k_{\Delta-G}$, k_{G-G}, $k_{\Delta-M}$, and k_{M-M}, were calculated from the slope of the curves.

approximately 0 (10 h for ΔoligoG and 2.5 h for ΔoligoM).

Decrease in the H-4 Δ signals correspond to cleavage of glycosidic linkages between a Δ and a saturated sugar residue. Assuming the time dependent degradation will follow first order kinetics, the rate of cleavage can be described by Eq. (I). The rate constant for cleavage of the Δ-G linkages, denoted $k_{\Delta-G}$, and the rate constant for cleavage of the Δ-M linkages, denoted $k_{\Delta-M}$, can be found by linear regression (Fig. 4 (A and C)).

^{1}H NMR resonances of H-4 Δ, H-1 internal residues and α and β reducing end signals were used to calculate the number average degree of polymerization (DP_n). In the case of ΔoligoM, the α reducing end signal was calculated using the α/β ratio (Aarstad et al., 2012), due to overlapping signals. Decrease in DP_n-1 corresponds to cleavage of glycosidic linkages between two saturated residues. Assuming the time dependent degradation will follow pseudo first order kinetics, the rate of cleavage can be described by Eq. (II). The rate constant for cleavage of the G-G linkages, denoted k_{G-G}, and the rate constant for cleavage of the M-M linkages, denoted k_{M-M}, can be found by linear regression (Fig. 4 (B and D)).

$$[A] = [A]_{t=0} \bullet e^{-kt} \quad \text{(I)}$$

$$\left(1 - \left(\frac{1}{DP_n - 1}\right)\right) = e^{-kt} \quad \text{(II)}$$

The rate constants $k_{\Delta-G}$, k_{G-G}, $k_{\Delta-M}$, and k_{M-M} determined from the slope of the curves (Fig. 4) are given in Table 1. Integration of signals at the start of the hydrolysis (0−2 h) of ΔoligoG was difficult due to overlapping signals and was therefore excluded from the calculations. However, this should not affect the estimated rate constants assuming the rate constants remains the same throughout the hydrolysis reaction.

The rate constants estimated from the hydrolysis of ΔoligoG were found to be $k_{\Delta-G} = 0.2993\ h^{-1}$ and $k_{G-G} = 0.0046\ h^{-1}$, meaning that the Δ-G linkages are cleaved approximately 65 times faster than the G-G linkages. Furthermore, the rate constants from the hydrolysis of ΔoligoM were found to be $k_{\Delta-M} = 1.5087\ h^{-1}$ and $k_{M-M} = 0.0351\ h^{-1}$. The ratio of hydrolysis rate for the Δ-M linkages to that of the M-M linkages was found to be approximately 43. We hypothesize that difference in hydrolysis rate is due to the stability of the intermediate in the hydrolysis reaction (Section 3.8). Notably, the reaction rate of cleavage of the Δ-M linkages was found to be 5 times faster compared to the Δ-G linkages. This agrees well with the fact that M-M linkages are more easily hydrolyzed compared to G-G linkages (Smidsrød et al., 1966; Smidsrød et al., 1967; Smidsrød et al., 1969). This result provides a complete picture on the order of selectivity for hydrolysis of alginate linkages: Δ-M > Δ-G > M-M ≈ G-M > M-G > G-G.

Table 1
Acid hydrolysis (pH* 3.4, 90 °C) of ΔoligoG and ΔoligoM was studied by time resolved NMR. The rate constants (k) are estimated based on first and pseudo first order kinetics.

Glycosidic linkage	k [h^{-1}]
Δ-G	0.2993
G-G	0.0046
Δ-M	1.5087
M-M	0.0351

3.3. Time-resolved ^{1}H NMR analysis showed the formation of three new products

Interestingly, during the time-resolved ^{1}H NMR analysis for

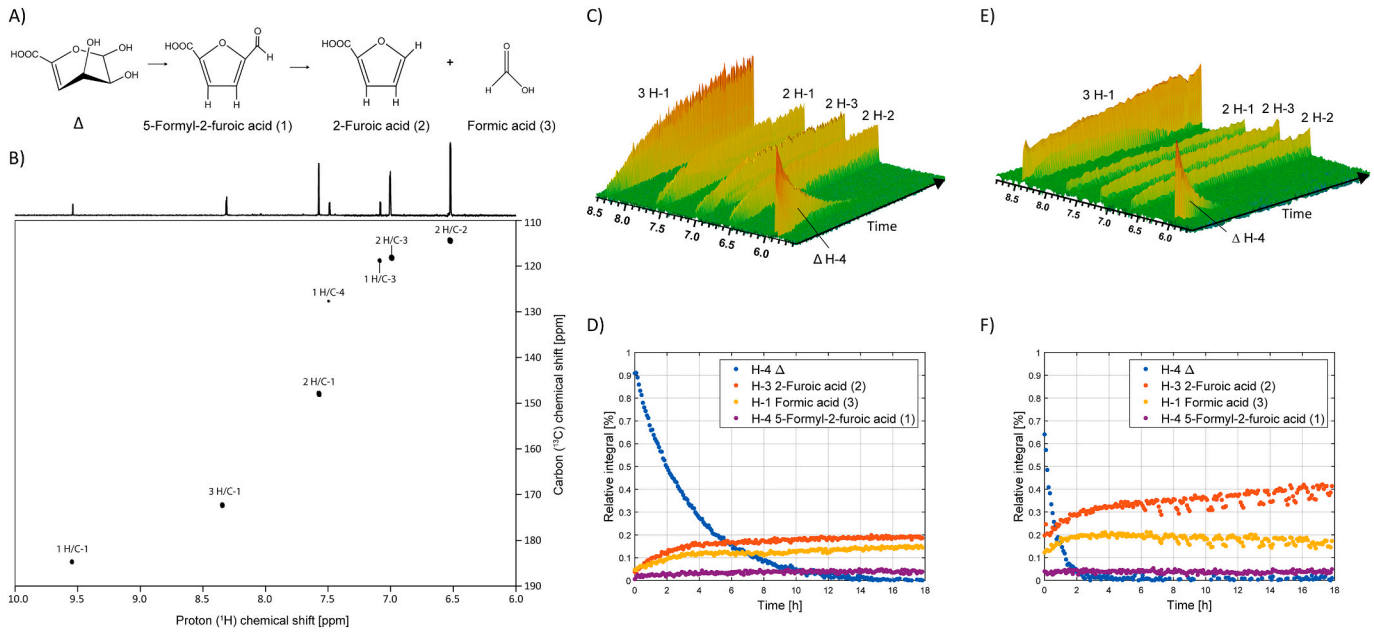

Fig. 5. NMR analysis of ΔoligoG and ΔoligoM during acid hydrolysis (pH* 3.4, 90 °C) showed three reaction products. A) Scheme detailing the formation of 5-formyl-2-furoic acid (1) from Δ and the formation of 2-furoic acid (2) and formic acid (1) from 5-formyl-2-furoic acid. B) Annotated $^{1}H—^{13}C$ HSQC spectrum showing the region of interest for reaction products obtained after acid hydrolysis (pH* 3.4, 90 °C) for approximately 21 h of ΔoligoG. C) ^{1}H NMR time-resolved spectra of ΔoligoG during acid hydrolysis (pH* 3.4, 90 °C). D) Relative integral [%] of the H-4, H-3, and H-1 signals of the three reaction products and Δ4G signal plotted as a function of time [h]. E) ^{1}H NMR time-resolved spectra of ΔoligoM during acid hydrolysis (pH* 3.4, 90 °C). F) Relative integral [%] of the H-4, H-3, and H-1 signals of the three reaction products and Δ4M signal plotted as a function of time [h].

estimation of rate constants, new signals appeared between 6.5 and 8.5 ppm for both ΔoligoG and ΔoligoM, indicating the formation of new products (Fig. 5 (C and E)). NMR analyses using various 2D NMR spectra resulted in assignment of a total of three new products. The first compound appearing was 5-formyl-2-furoic acid (1). Under the examined reaction conditions (pH* 3.4, 90 °C), the 5-formyl-2-furoic acid was further degraded to 2-furoic acid (2) and formic acid (3) (Fig. 5 (A and B), see Tables S2 and S3 in the supplementary material for chemical shift assignment). A proposed mechanism for the acid conversion of Δ from alginate oligosaccharides is described in Section 3.4 below. The relative integrals [%] of H-4 Δ, H-3 2-furoic acid, H-1 formic acid and H-4 5-formyl-2-furoic acid of ΔoligoG and ΔoligoM as a function of time is shown in Fig. 5 (D and F).

3.4. *Proposed mechanism for acid conversion of Δ*

It has previously been described how Δ from alginate in water under neutral or alkaline conditions is converted to DEH and DHF through a base-catalyzed mechanism (Arntzen et al., 2021) or by the enzyme KdgF (Hobbs et al., 2016) by the mechanism described by Rønne et al. (in press). However, formation of 5-formyl-2-furoic acid, 2-furoic acid, and formic acid when degrading Δ has not been previously described. In Section 3.3., it was shown how these three compounds were all formed under acid hydrolysis (pH* 3.4) at high temperature.

Rosenau and colleagues (Rosenau et al., 2017) described synthesis of model compounds of hexeneuronic acid, where a Δ-like compound *O*-methylated at the anomeric position was synthesized and then degraded using high temperature and low pH to imitate conditions under pulping of cellulose. The degradation of the Δ-like compound resulted in formation of the same three compounds as was observed in this study: 5-formyl-2-furoic acid, 2-furoic acid, and formic acid.

In Fig. 6, a mechanism for formation of 5-formyl-2-furoic acid, 2-furoic acid, and formic acid is proposed. As the reaction analysis was performed in D_2O, the mechanism was described accordingly. The first step of the mechanism is hydrolysis of the glycosidic bond, for which further discussion will follow in Section 3.8. The second step is an acid-catalyzed linearization of Δ forming DEH. The third step is a ring closure forming DHF. In the fourth step, a condensation reaction of DHF results in 5-formyl-2-furoic acid, which was observed as small signals in NMR. The fifth step is the loss of the aldehyde forming 2-furoic acid and formic acid. The mechanism shows that at low pH and high temperature, the degradation of Δ does not stop at DEH and DHF (as observed at neutral or alkaline conditions), but DEH and DHF are simply intermediates in the acid hydrolysis.

With time-resolved NMR spectroscopy it was possible to observe the signal increase over time of these three new compounds. The signal integrals of the new compounds did not amount to the same integral as for the disappearing Δ signals (see Fig. 5). This could be due to Δ being protonated, while 5-formyl-2-furoic acid and 2-furoic acid are mainly deuterated, as the reaction is taking place in D_2O. Following the proposed mechanism only the C-3 position of 2-furoic acid should be able to be deuterated, but H-3 and H-2 are of equal low signal intensity, so both C-3 and C-2 must be somewhat deuterated. This can be explained by the compound being able to tautomerize as shown in step 6) in Fig. 6. The reaction in step 6) can also occur in the other direction towards C-3.

The proposed mechanism in Fig. 6 is based on our experimental NMR data, knowledge of the base-catalyzed degradation of Δ (Arntzen et al., 2021; Rønne, et al. (in press)), and the observations for rearrangement of

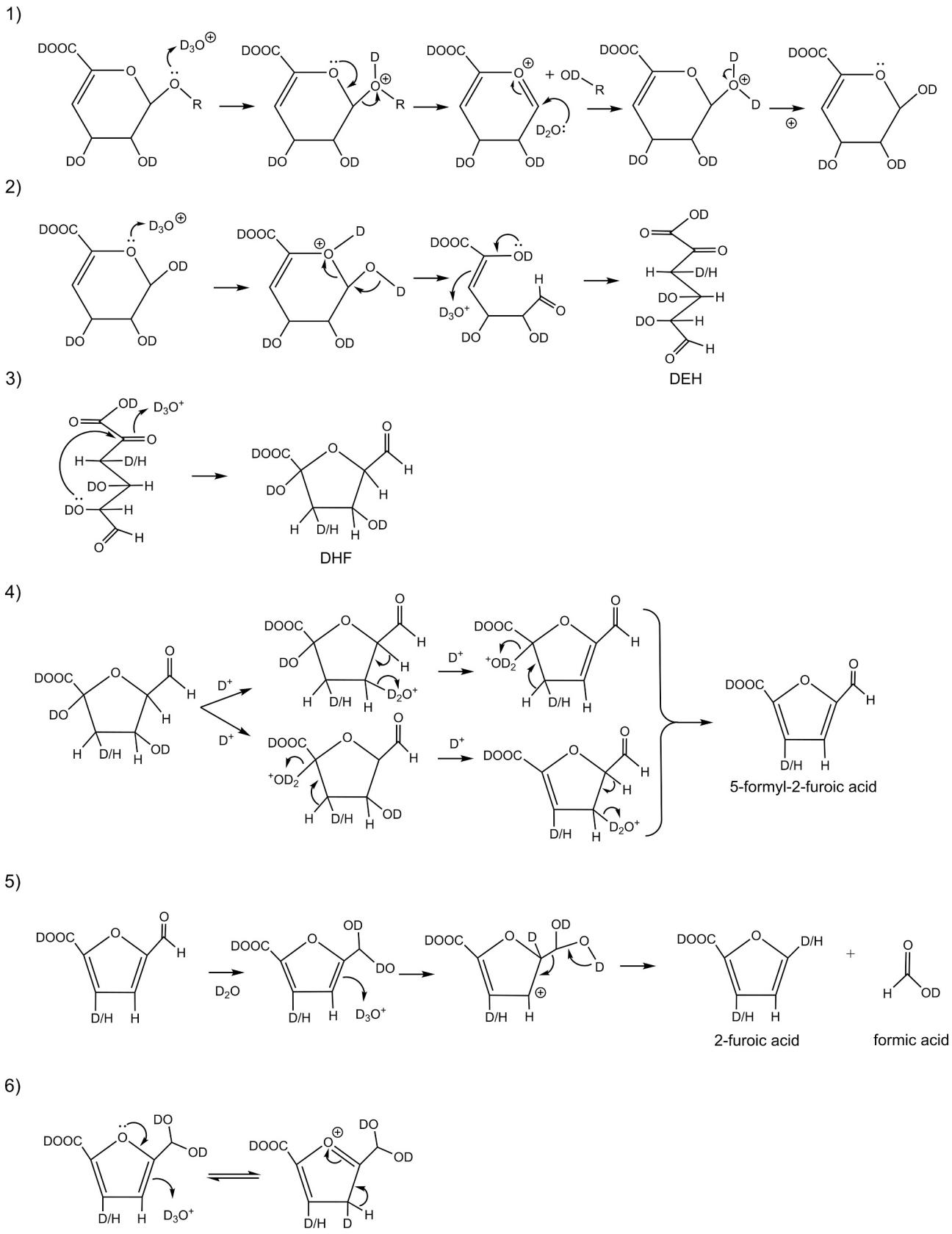

Fig. 6. Scheme detailing the hydrolysis of the *O*-glycosidic bond at the non-reducing end of alginate releasing Δ and further degradation of Δ to 5-formyl-2-furoic acid, 2-furoic acid and formic acid, which were all observed with NMR. The proposed mechanism includes five key steps: 1) hydrolysis of the *O*-glycosidic bond, 2) linearization of Δ forming DEH, 3) ring closure forming DHF, 4) condensation forming 5-formyl-2-furoic acid, and 5) loss of aldehyde forming 2-furoic acid and formic acid. After product formation tautomerization (6) takes place explaining the deuteration of both C-2 and C-3 of 2-furoic acid.

hexose under acidic conditions (Rosenau et al., 2017). Rosenau et al. (2017) described a less detailed mechanism for the conversion of the Δ-like compound to 5-formyl-2-furoic acid containing the same key steps as described here. They observed the DEH and DHF intermediates using NMR and isotopically labelled starting materials, which further confirms the key steps of the proposed mechanism.

3.5. Monomeric Δ generated by an exolyase undergoes the same reaction scheme under acidic conditions

To study if acid hydrolysis of Δ monosaccharides under the same reaction conditions resulted in the same reaction products as shown in Fig. 5, degradation of polyM using an exolyase was performed. PolyM was enzymatically degraded with AlyA3 (Jouanneau et al., 2021) exolyase for approximately 1 h before the lyase reaction was stopped by decreasing the pH* to 3.6 and an acid hydrolysis was performed at 90 °C. The reaction was monitored using time-resolved ^{1}H NMR. The ^{1}H NMR spectra showed the appearance of new signals corresponding to the same reaction products elucidated for ΔoligoG and ΔoligoM. Hence, the same reaction products are being produced after an acid hydrolysis of monomeric Δ, as for Δ directly cleaved off an alginate oligosaccharide treated with an endolyase. Time-resolved ^{1}H NMR spectra and an annotated ^{1}H—^{13}C HSQC spectrum can be found in supplementary information, Fig. S4.

3.6. Chemo-enzymatic preparation of saturated guluronic acid oligosaccharides starting from polyM

With these experiments, we aim to demonstrate how the chemo-enzymatic method is superior in the production of α-L-guluronate oligosaccharides with a lower content of β-D-mannuronate residues compared to what can be achieved using chemical depolymerization alone by using polyM as starting material. Alginate lyases can be specific towards different glycosidic linkages. By degrading an alginate material containing a mixture of block structures with a M-lyase that is M-M and G-M specific, M-rich regions can be removed from the sample using acid precipitation. Furthermore, when a G-M linkage is cleaved, the M residue at the newly formed non-reducing end is converted to Δ, which can be chemically removed by acid hydrolysis, further increasing F_G.

^{1}H NMR spectra of alginate samples from the different steps in the process are shown in Fig. 7. Corresponding HPAEC-PAD chromatograms can be found in Fig. S5-S6 in supplementary material. First, PolyM was epimerized with the mannuronan C-5 epimerase AlgE6 to F_G = 0.51. Thereafter, the sample was treated with M-lyase (M-M/G-M specific)

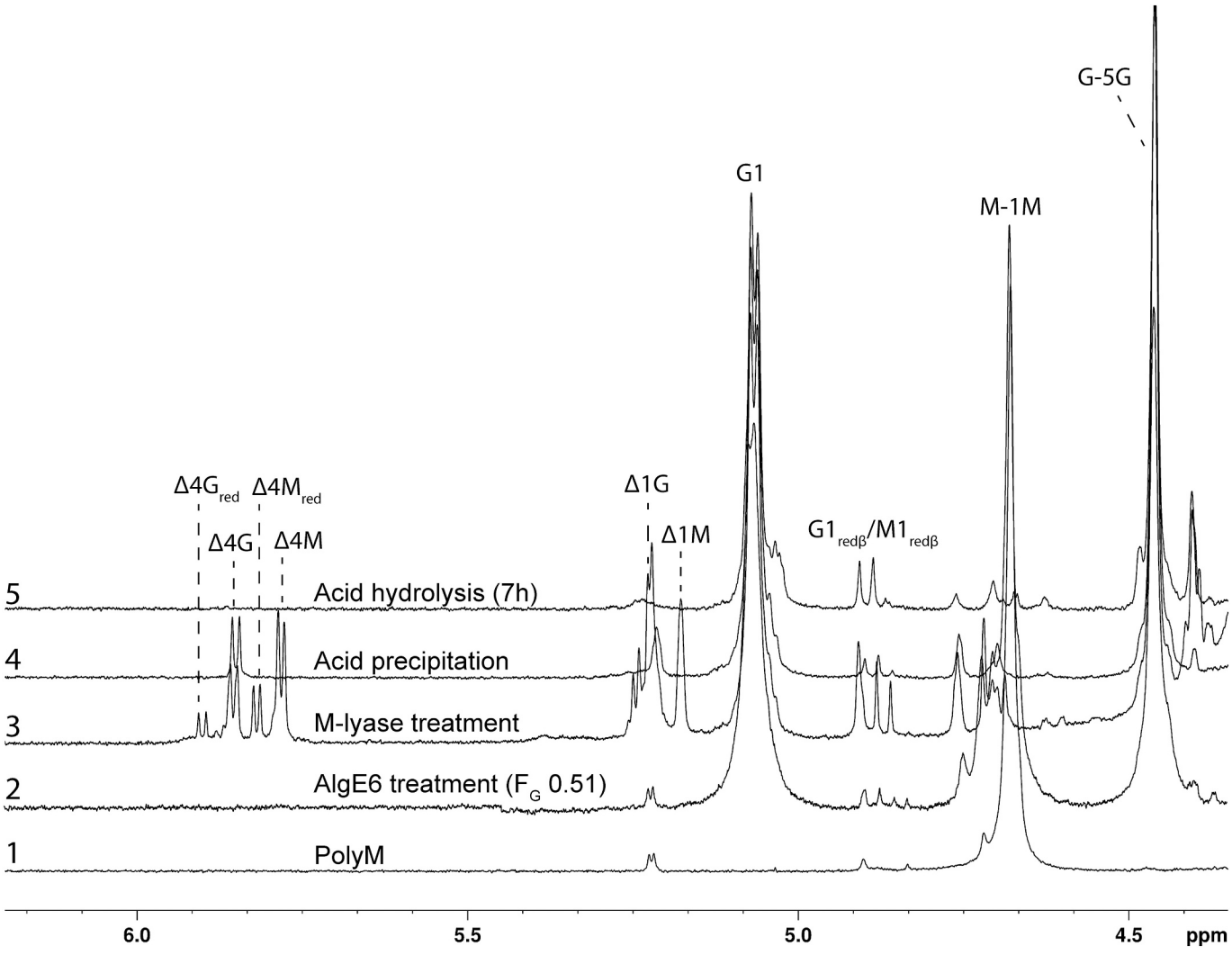

Fig. 7. ^{1}H NMR spectra of 1) polyM, 2) epimerization of polyM with AlgE6 to F_G 0.51, 3) lyase degradation using *H. tuberculata* M-lyase (M-M/G-M specific), 4) insoluble fraction after acid precipitation at pH 3.1 and 5) precipitate after dissolution by neutralization followed by 7 h hydrolysis at 90 °C, pH 3.6.

resulting in oligosaccharides with a Δ at the non-reducing end. The result of the lyase reaction is clearly seen in the ^{1}H NMR spectrum by the 4 doublets that have appeared at 5.75–5.90 ppm, which corresponds to $\Delta4G_{red}$ (5.90 ppm), Δ4G (5.85 ppm), $\Delta4M_{red}$ (5.82 ppm), and Δ4M (5.78 ppm) (Aarstad et al., 2012).

Furthermore, an acid precipitation step was performed to remove small M-rich oligosaccharides, and M and G dimers ($\Delta4G_{red}$ and $\Delta4M_{red}$), the effect of which was confirmed by the disappearance of the Δ4M peak, as well as the $\Delta4G_{red}/M_{red}$ dimer peaks in the ^{1}H NMR spectrum. Finally, an acid hydrolysis step (95 °C, pH 3.6) for 7 h resulted in the disappearance of the Δ4G resonance peak, indicating removal of Δ at the non-reducing end of the oligosaccharides. The final product generated by the process described was saturated oligoG ($DP_n = 10.3$) with an $F_G > 0.95$.

3.7. Acid hydrolysis of polygalacturonic acid and heparin showed that the chemo-enzymatic method works for other uronic acid-containing polysaccharides

To demonstrate that the chemo-enzymatic method is general for uronic acid-containing polysaccharides, lyase degraded polygalacturonic acid and heparin were acid hydrolyzed under the same conditions as previously described for alginate (Section 3.3). The acid hydrolysis reactions (pH* 3.4, 90 °C) were performed directly in an NMR tube while monitoring the reactions by recording a ^{1}H NMR spectrum every five minutes (Fig. 8.) to confirm the chemical removal of Δ at the non-reducing ends. The resonance peak corresponding to the H4Δ (polygalacturonic acid ~5.9 ppm; heparin ~6.2 ppm) decreased during both hydrolysis reactions, indicating that the unsaturated residue at the non-reducing end is cleaved off the oligosaccharide. These results strengthen our hypothesis that the described method works for other uronic acid-containing polysaccharides after lyase degradation. We hypothesize that this is due to the stability of the intermediate, which is further explained in Section 3.8. The conversion products from Δ under these conditions are not the same as for alginate due to differences in molecular structure. However, the key finding from this experiment is that the Δ is removed from the oligosaccharides by acid hydrolysis. In the case of heparin, the relative integral of the H4Δ signal does not reach 0 %, due to the H4Δ signal overlapping with another signal.

3.8. Intermediate structures in the hydrolysis of the glycosidic bond

Our hypothesis is based on the difference in stability of the intermediate structures in the hydrolysis of a glycosidic bond between two saturated uronic acid residues compared to a glycosidic bond between Δ and a saturated uronic acid residue. In Fig. 9, we propose mechanisms for the hydrolysis of the glycosidic bond between two saturated uronic acids (1) and for the hydrolysis of the glycosidic bond between Δ and a saturated uronic acid (2). In both mechanism 1 and 2, an intermediate is formed containing a positive charge and a double bond. However, in mechanism 2, the non-reducing end sugar residue has a double bond between C4 and C5, hence the intermediate has conjugated double bonds, making it a more stable (energetically favorable) intermediate compared to the one formed in mechanism 1. The activation energy of this intermediate (mechanism 2) is therefore lower compared to the intermediate in mechanism 1, which likely results in the higher reaction rate.

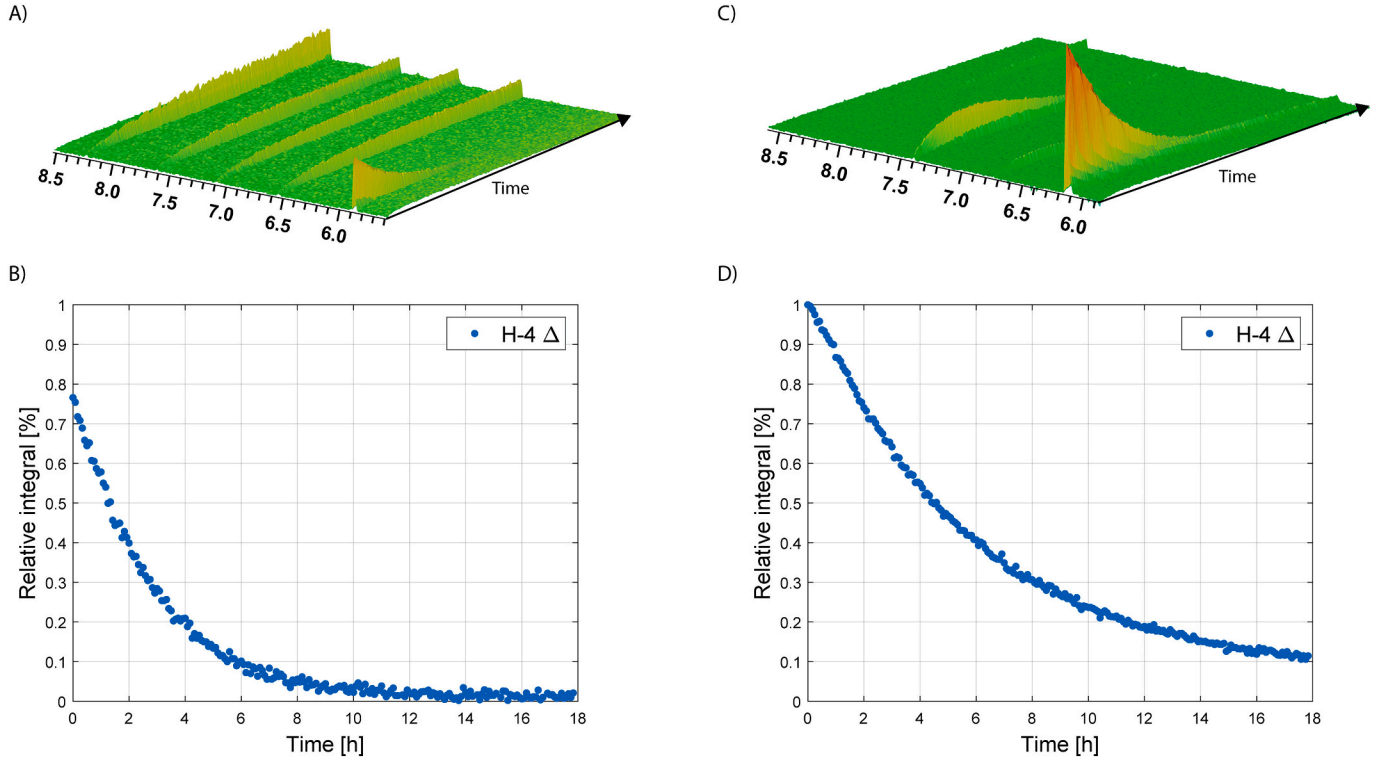

Fig. 8. A) ^{1}H NMR time-resolved spectra of unsaturated polygalacturonic acid during acid hydrolysis (pH* 3.4, 90 °C). B) Relative integral [%] of the H-4 Δ signal (polygalacturonic acid ~5.9 ppm) plotted as a function of time [h]. C) ^{1}H NMR time-resolved spectra of unsaturated heparin during acid hydrolysis (pH* 3.4, 90 °C). D) Relative integral [%] of the H-4 Δ signal (heparin ~6.2 ppm) plotted as a function of time [h].

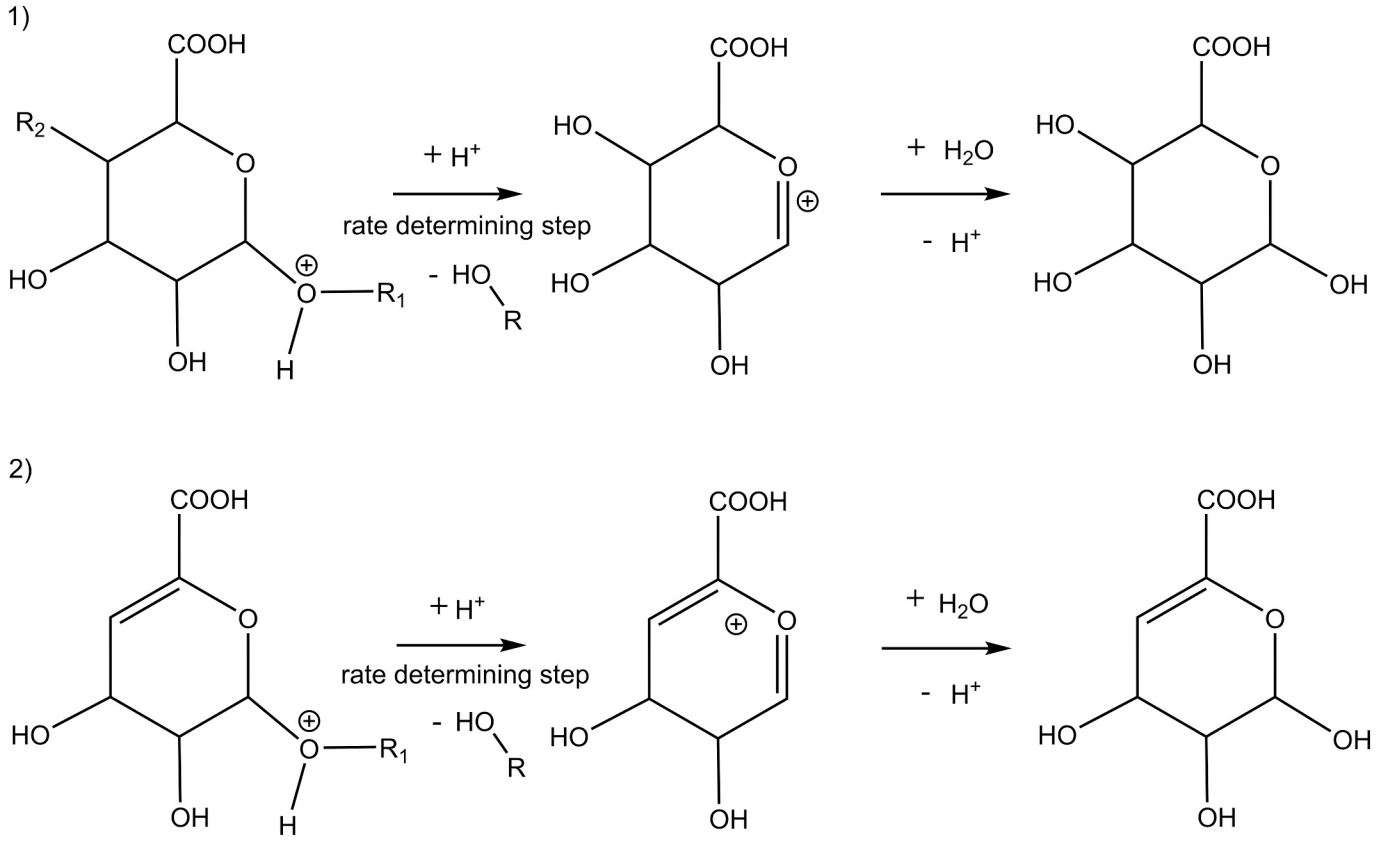

Fig. 9. Intermediate structures in the hydrolysis of the glycosidic bond between two saturated residues (1) and between an unsaturated and a saturated residue (2). In both mechanisms an intermediate structure containing a positive charge on the oxygen atom and a double bond is formed. In mechanism 2, the hydrolysis of the unsaturated sugar (Δ) on the non-reducing end results in an intermediate structure with conjugated double bonds which makes the intermediate in mechanism 2 more stable than the intermediate in mechanism 1. R_1 is another uronic acid residue. R_2 is OH in the case of alginate or polygalacturonic acid, or $NHS(=O)_2(OH)$/$OS(=O)_2(OH)$ in the case of heparin. The carboxylic acid could also be $OS(=O)_2(OH)$ in the case of heparin.

4. Conclusions

The method presented in this paper describes the removal of Δ residues from the non-reducing end after lyase-degradation of uronic acid-containing oligosaccharides (alginate, heparin, and polygalacturonic acid). This allows for utilizing specific lyases-catalyzing β-elimination reactions for the preparation of saturated uronic acid-containing oligosaccharides. In-depth studies of alginate substrates revealed that the reaction rate for hydrolysis of the Δ-G linkages was found to be 65 times higher than of G-G linkages, and the reaction rate for hydrolysis of the Δ-M linkages was found to be 43 times higher than of M-M linkages at pH* 3.4, 90 °C. These results strengthen our hypothesis that glycosidic linkages with Δ on the non-reducing end hydrolyze at a higher rate compared to the hydrolysis of a glycosidic linkage between two saturated uronic acid sugar residues. Furthermore, it was shown that the removal of the Δ residue from the non-reducing end of alginate oligosaccharides at pH* 3.4 and 90 °C resulted in the formation of three reaction products: 5-formyl-2 furoic acid, 2-furoic acid and formic acid.

Funding

The work was funded by the Research Council of Norway through projects #332416 (TARRGET), #315385 (AlgModE), #309558 (SFI-IB), #226244 (NNP-Norwegian NMR Platform), #228542/O30 (Tailored OligoG in the treatment of chronic infectious biofilms) and SO stipend from NTNU.

CRediT authorship contribution statement

Mina Gravdahl: Writing – review & editing, Writing – original draft, Visualization, Methodology, Investigation, Formal analysis, Conceptualization. **Olav A. Aarstad:** Writing – review & editing, Methodology, Investigation, Formal analysis, Conceptualization. **Agnes B. Petersen:** Writing – review & editing, Visualization, Methodology, Investigation. **Stina G. Karlsen:** Investigation. **Ivan Donati:** Writing – review & editing, Investigation. **Mirjam Czjzek:** Writing – review & editing, Investigation. **Ove Alexander Høgmoen Åstrand:** Writing – review & editing, Funding acquisition. **Philip D. Rye:** Writing – review & editing, Funding acquisition. **Anne Tøndervik:** Writing – review & editing, Funding acquisition. **Håvard Sletta:** Writing – review & editing, Funding acquisition, Conceptualization. **Finn L. Aachmann:** Writing – review & editing, Supervision, Project administration, Methodology, Investigation, Funding acquisition, Formal analysis, Conceptualization. **Gudmund Skjåk-Bræk:** Writing – review & editing, Funding acquisition, Conceptualization.

Declaration of competing interest

The authors declare that they have no known competing financial interests or personal relationships that could have appeared to influence the work reported in this article.

Data availability

Data will be made available on request.

Acknowledgements

The authors would like to thank Wenche I. Strand for valuable discussions on alginate ^{1}H NMR.

Appendix A. Supplementary data

Supplementary data to this article can be found online at https://doi.org/10.1016/j.carbpol.2024.122487.

References

Aarstad, O. A., Strand, B. L., Klepp-Andersen, L. M., & Skjåk-Bræk, G. (2013). Analysis of G-block distributions and their impact on gel properties of in vitro epimerized mannuronan. *Biomacromolecules, 14*(10), 3409–3416.

Aarstad, O. A., Tøndervik, A., Sletta, H., & Skjåk-Bræk, G. (2012). Alginate sequencing: An analysis of block distribution in alginates using specific alginate degrading enzymes. *Biomacromolecules, 13*(1), 106–116.

Arntzen, M. O., Pedersen, B., Klau, L. J., Stokke, R., Oftebro, M., Antonsen, S. G., … Eijsink, V. G. H. (2021). Alginate degradation: Insights obtained through characterization of a thermophilic exolytic alginate lyase. *Applied and Environmental Microbiology, 87*(6).

Caffall, K. H., & Mohnen, D. (2009). The structure, function, and biosynthesis of plant cell wall pectic polysaccharides. *Carbohydrate Research, 344*(14), 1879–1900.

Casu, B., & Lindahl, U. (2001). Structure and biological interactions of heparin and heparan sulfate. *Advances in Carbohydrate Chemistry and Biochemistry, 57*, 159–206.

Coultate, T. P. (2016). *Food: The chemistry of its components* (6th ed.) London, (Chapter 2).

Ermund, A., Recktenwald, C. V., Skjåk-Bræk, G., Meiss, L. N., Onsøyen, E., Rye, P. D., … Hansson, G. C. (2017). OligoG CF-5/20 normalizes cystic fibrosis mucus by chelating calcium. *Clinical and Experimental Pharmacology and Physiology, 44*(6), 639–647.

Falkeborg, M., Cheong, L. Z., Gianfico, C., Sztukiel, K. M., Kristensen, K., Glasius, M., … Guo, Z. (2014). Alginate oligosaccharides: Enzymatic preparation and antioxidant property evaluation. *Food Chemistry, 164*, 185–194.

Gimmestad, M., Sletta, H., Ertesvåg, H., Bakkevig, K., Jain, S., Suh, S., … Valla, S. (2003). The Pseudomonas fluorescens AlgG protein, but not its mannuronan C-5-epimerase activity, is needed for alginate polymer formation. *Journal of Bacteriology, 185*(12), 3515–3523.

Gorin, P., & Spencer, J. F. T. (1966). Exocellular alginic acid from *Azotobacter Vinelandii*. *Canadian Journal of Chemistry, 44*, 993–998.

Grant, T. G., Morris, R. E., Rees, A. D., Smith, J. P., & Thom, D. (1973). Biological interactions between polysaccharides and divalent cations: The egg-box model. *FEBS Letters, 32*, 195–198.

Haug, A., Larsen, B., & Smidsrød, O. (1967). Studies of the sequence of uronic acid residues in alginic acid. *Acta Chemica Scandinavica, 21*, 691–704.

Hobbs, J. K., Lee, S. M., Robb, M., Hof, F., Barr, C., Abe, K. T., … Boraston, A. B. (2016). KdgF, the missing link in the microbial metabolism of uronate sugars from pectin and alginate. *Proceedings of the National Academy of Sciences of the United States of America, 113*(22), 6188–6193.

Holtan, S., Bruheim, P., & Skjåk-Bræk, G. (2006). Mode of action and subsite studies of the guluronan block-forming mannuronan C-5 epimerases AlgE1 and AlgE6. *Biochemical Journal, 395*, 319–329.

Holtan, S., Zhang, Q. J., Strand, W. I., & Skjåk-Bræk, G. (2006). Characterization of the hydrolysis mechanism of polyalternating alginate in weak acid and assignment of the resulting MG-oligosaccharides by NMR spectroscopy and ESI-mass spectrometry. *Biomacromolecules, 7*(7), 2108–2121.

Jouanneau, D., Klau, L. J., Larocque, R., Jaffrennou, A., Duval, G., le Duff, N., … Thomas, F. (2021). Structure – Function analysis of a new PL17 oligoalginate lyase from the marine bacterium *Zobellia galactanivorans* Dsij. *Glycobiology, 31*(10), 1364–1377.

Linker, A., & Jones, R. S. (1966). A new polysaccharide resembling alginic acid isolated from pseudomonads. *The Journal of Biological Chemistry, 241*(16), 3845–3851.

Powell, L. C., Adams, J. Y. M., Quoraishi, S., Py, C., Oger, A., Gazze, S. A., … Thomas, D. W. (2023). Alginate oligosaccharides enhance the antifungal activity of nystatin against candidal biofilms. *Frontiers in Cellular and Infection Microbiology, 13*.

Pritchard, M. F., Powell, L. C., Khan, S., Griffiths, P. C., Mansour, O. T., Schweins, R., … Ferguson, E. L. (2017). The antimicrobial effects of the alginate oligomer OligoG CF-5/20 are independent of direct bacterial cell membrane disruption. *Scientific Reports, 7*.

Pritchard, M. F., Powell, L. C., Menzies, G. E., Lewis, P. D., Hawkins, K., Wright, C., … Thomas, D. W. (2016). A new class of safe oligosaccharide polymer therapy to modify the mucus barrier of chronic respiratory disease. *Molecular Pharmaceutics, 13*(3), 863–872.

Rønne, M. E., Andersen, C. D., Teze, D., Petersen, A. B., Fredslund, F., Stender, E. G. P., Chaberski, E. K., Holck, J., Aachmann, F. L., Welner, D. & Birte Svensson (in press). Action and cooperation in alginate degradation by three enzymes from the human gut bacterium Bacteroides eggerthii DSM 20697. Journal of Biological Chemistry.

Rosenau, T., Potthast, A., Zwirchmayr, N. S., Hosoya, T., Hettegger, H., Bacher, M., … Dietz, T. (2017). Chromophores from hexeneuronic acids (HexA): Synthesis of model compounds and primary degradation intermediates. *Cellulose, 24*(9), 3703–3723.

Shriver, Z., Capila, I., Venkataraman, G., & Sasisekharan, R. (2012). Heparin and heparan sulfate: Analyzing structure and microheterogeneity. *Handbook of Experimental Pharmacology, 207*, 159–176.

Smidsrød, O., Haug, A., & Larsen, B. (1966). Influence of Ph on rate of hydrolysis of acidic polysaccharides. *Acta Chemica Scandinavica, 20*(4), 1026–1034.

Smidsrød, O., Larsen, B., & Haug, A. (1967). Acid hydrolysis of polysaccharides containing uronic acid residues. *Carbohydrate Research, 5*, 371–372.

Smidsrød, O., Larsen, B., Painter, T., & Haug, A. (1969). The role of intramolecular autocatalysis in acid hydrolysis of polysaccharides containing 1,4-linked hexuronic acid. *Acta Chemica Scandinavica, 23*(5), 1573–1580.

Solberg, A., Mo, I. V., Aachmann, F. L., Schatz, C., & Christensen, B. E. (2021). Alginate-based diblock polymers: Preparation, characterization and Ca-induced self-assembly. *Polymer Chemistry, 12*(38).

Solberg, A., Mo, I. V., Omtvedt, L. A., Strand, B. L., Aachmann, F. L., Schatz, C., & Christensen, B. E. (2022). Carbohydr Polym Special Issue Invited contribution: Click chemistry for block polysaccharides with dihydrazide and dioxyamine linkers - A review. *Carbohydrate Polymers*, 278.

Tøndervik, A., Aarstad, O. A., Aune, R., Maleki, S., Rye, P. D., Dessen, A., … Sletta, H. (2020). Exploiting Mannuronan C-5 epimerases in commercial alginate production. *Marine Drugs, 18*(11), 565.

Wardrop, D., & Keeling, D. (2008). The story of the discovery of heparin and warfarin. *British Journal of Haematology, 141*, 757–763.

Wishart, D. S., Bigam, C. G., Yao, J., Abildgaard, F., Dyson, H. J., Oldfield, E., … Sykes, B. D. (1995). H-1, C-13 and N-15 chemical-shift referencing in biomolecular NMR. *Journal of Biomolecular NMR, 6*(2), 135–140.